Am J Cancer Res 2026;16(7):3136-3149
www.ajcr.us /ISSN:2156-6976/ajcr0173264

Original Article

CAAP1 suppresses tumor growth and metastasis via interacting with EIF3I in high-grade serous ovarian carcinoma

Chunyan Wang[1,2,3,4*], Liyang Liang[5*], Lei Kuang[1,2,3,4], Sisi Liu[1,2,3,4], Weiwei Qian[1,2,3,4], Chunlei Zhang[5]

[1]Department of Gynecology, The Affiliated Lianyungang Hospital of Xuzhou Medical University/The First People's Hospital of Lianyungang, Lianyungang, Jiangsu, China; [2]Department of Gynecology, The First Affiliated Hospital of Kangda College of Nanjing Medical University/The First People's Hospital of Lianyungang, Lianyungang, Jiangsu, China; [3]Department of Gynecology, Lianyungang Clinical College of Nanjing Medical University/The First People's Hospital of Lianyungang, Lianyungang, Jiangsu, China; [4]Department of Gynecology, The First People's Hospital of Lianyungang, Lianyungang, Jiangsu, China; [5]Department of Orthopedics, Nanjing Hospital of Chinese Medicine Affiliated to Nanjing University of Chinese Medicine, Nanjing, Jiangsu, China. [*]Equal contributors and co-first authors.

Received April 13, 2026; Accepted July 8, 2026; Epub July 15, 2026; Published July 30, 2026

Abstract: High-grade serous ovarian cancer (HGSOC) is frequently diagnosed at advanced stages with refractory peritoneal metastases, resulting in a dismal prognosis. Caspase activity and apoptosis inhibitor 1 (CAAP1), an apoptosis regulator with debated functions, has an unexplored role in HGSOC progression. Herein, the prognostic value of CAAP1 was evaluated using The Cancer Genome Atlas (TCGA) database and clinical tissue samples. The effects of CAAP1 on HGSOC cell proliferation, migration, and apoptosis resistance were examined via cell counting kit-8 (CCK-8) and 5-Ethynyl-2'-deoxyuridine (EdU) incorporation, wound healing, Transwell, and terminal deoxynucleotidyl transferase dUTP nick end labeling (TUNEL) assays. A subcutaneous xenograft model was employed to verify the tumor-suppressive role of CAAP1 in vivo. Furthermore, liquid chromatography-tandem mass spectrometry (LC-MS/MS) and co-immunoprecipitation (Co-IP) were performed to identify and validate CAAP1-interacting proteins, with Western blotting utilized to assess downstream signaling alterations. Our results demonstrated that CAAP1 downregulation was significantly correlated with poor prognosis in HGSOC patients. Functionally, CAAP1 knockdown promoted HGSOC cell proliferation, migration, and apoptosis resistance, whereas CAAP1 overexpression exerted opposite inhibitory effects. In vivo experiments corroborated that CAAP1 overexpression effectively suppressed tumor growth. Mechanistically, CAAP1 was found to interact with eukaryotic translation initiation factor 3 subunit I (EIF3I) to modulate the expression of cancer-related proteins. Collectively, this study establishes that CAAP1 functions as a tumor suppressor in HGSOC by binding to EIF3I, thereby restraining tumor growth and metastasis.

Keywords: HGSOC, CAAP1, EIF3I, tumor suppressor

Introduction

Ovarian cancer (OC) is a common malignant tumor of the female reproductive system, with HGSOC being the most aggressive subtype [1]. HGSOC accouns for approximately 80% of OC-related deaths and demonstrats an extremely poor clinical prognosis [2]. The five-year survival rate in advanced-stage patients is typically less than 30%, with the primary cause of treatment failure being extensive peritoneal metastasis [3]. According to statistics, approximately 70% of patients already have intra-abdominal dissemination at the time of initial diagnosis. Although most patients achieve initial remission through cytoreductive surgery combined with platinum-based chemotherapy, over 70% will eventually experience recurrence with intraperitoneal seeding [4].

Currently, the specific molecular mechanisms of HGSOC peritoneal dissemination remain unclear. The key regulators and signaling pathways controlling the metastatic cascade of HGSOC, including tumor cell detachment, spheroid formation, anoikis resistance, and peritoneal colonization, are still undefined [5-7].

This gap in knowledge confines current therapies, primarily cytoreductive surgery and platinum-based chemotherapy, to targeting existing tumors, without effective approach to disrupt metastasis and prevent recurrence. Therefore, deciphering the molecular mechanisms underlying HGSOC metastasis and colonization is essential for advancing therapeutic progress, overcoming existing bottlenecks, and improving clinical outcomes.

CAAP1 was initially identified as an apoptosis regulator, yet a consensus on its precise biological function remains elusive. Early studies demonstrated that CAAP1 knockdown enhanced caspase activation in specific cancer cell lines, suggesting an anti-apoptotic role [8, 9]. However, subsequent research revealed that CAAP1 depletion impaired DNA damage-induced apoptosis, indicating that its function may be context-dependent and potentially even pro-apoptotic [10, 11]. This controversy highlights the complex relationship between CAAP1 and apoptosis, suggesting its role likely varies depending on cell type and microenvironment. Notably, the role of CAAP1 in tumor progression also exhibits significant cancer-type specificity. For instance, in colorectal cancer and hepatoma, CAAP1 has been shown to promote cell proliferation, migration, and chemotherapy resistance, functioning as a potential oncogene [9, 12]. Conversely, other study have suggested that CAAP1 may increase chemosensitivity in OC cells [13]. However, whether CAAP1 influences HGSOC progression remains unexplored.

Based on bioinformatics analysis of TCGA database, this study identified CAAP1 as an independent protective factor in HGSOC. Subsequently, the clinical significance and value of CAAP1 were evaluated by clinical tissue samples. Finally, through in vitro and in vivo functional experiments, it was confirmed that CAAP1 effectively inhibits the proliferation, metastasis, and anti-apoptotic capacity of HGSOC cells. This study reveals the tumor-suppressive function of CAAP1 in HGSOC, providing an important theoretical basis for understanding the molecular mechanisms of HGSOC progression and for exploring potential therapeutic strategies.

Materials and methods

Data acquisition and bioinformatics analysis

RNA sequencing data of 204 serous ovarian carcinoma (SOC) samples were obtained from TCGA database (https://portal.gdc.cancer.gov). Genome-wide univariate Cox regression analysis was performed to identify genes significantly associated with prognosis. Survival analysis was conducted using the median expression level of each gene as the cut-off value. All statistical computations were carried out in R software (version 4.0.3).

Clinical samples

A cohort of 71 paired HGSOC and adjacent normal ovarian tissue (located at least 5 cm from the carcinoma focus) samples were collected from patients who underwent primary cytoreductive surgery at the First People's Hospital of Lianyungang. All cases were pathologically confirmed as HGSOC and had complete clinicopathological and follow-up data. Freshly resected tissue specimens were either snap-frozen in liquid nitrogen or processed as formalin-fixed paraffin-embedded blocks. The study was conducted in accordance with the Declaration of Helsinki, approved by the Institutional Review Board of the First People's Hospital of Lianyungang (NO. KY-2025060-4002-1, June 6, 2025) and written informed consent was obtained from all participants prior to inclusion.

Cell lines and culture conditions

The HGSOC cell lines OV-90 and OVCAR3, the low-grade serous ovarian cancer (LGSOC) cell line HO-8910, the ovarian adenocarcinoma cell line SKOV3 (of controversial origin), and the normal ovarian epithelial cell line IOSE-80 were purchased from the American Type Culture Collection (ATCC). OV-90 and OVCAR3 cells were maintained in RPMI-1640 medium supplemented with 10% fetal bovine serum (FBS) and 1% penicillin/streptomycin. IOSE-80 cells were cultured in DMEM with 10% FBS. SKOV3 cells were cultured in McCoy's 5A medium supplemented with 10% FBS and 1% penicillin/streptomycin. All cultures were maintained at 37°C in a 5% CO_2 atmosphere. All cell lines were authenticated by short tandem

repeat profiling and tested negative for mycoplasma contamination.

Antibodies

Primary antibodies against CAAP1 (Thermo Fisher Scientific, PA5-54956, 1:6000), EIF3I (Proteintech, 85603-2-RR, 1:10000), Cyclin D1 (Proteintech, 60186-1-Ig, 1:40000), c-Myc (Proteintech, 10828-1-AP, 1:12000), E-cadherin (Proteintech, 20874-1-AP; 1:5000), N-cadherin (Proteintech, 22018-1-AP; 1:3000), vimentin (Proteintech, 10366-1-AP, 1:4000), GAPDH (Proteintech, 60004-1-Ig, 1:10000), Actin (Proteintech, 66009-1-Ig, 1:10000) and, β-Tubulin (Proteintech, 10094-1-AP, 1:6000) and 6*His, His-Tag (Proteintech, 84814-1-RR, 1:3000) were used for Western blot and immunoprecipitation. HRP-conjugated goat anti-rabbit IgG (H+L) secondary antibody (Proteintech, RGAR001, 1:50000) and HRP-conjugated goat anti-mouse IgG (H+L) secondary antibody (Proteintech, RGAM001, 1:20000) were used for Western blot.

Plasmid construction and lentiviral transfection

For CAAP1 overexpression, the full-length CAAP1 coding sequence was PCR-amplified and cloned into the CMV promoter region of the pSLenti-U6-shRNA(NC2)-CMV-F2A-Puro-WPRE lentiviral vector (Heyuan Liji (Shanghai) Biotechnology Co., Ltd.) (where the U6 promoter drives a non-targeting control shRNA, NC2). For CAAP1 knockdown, specific short hairpin RNA (shRNA) sequences targeting CAAP1 were designed, annealed, and inserted into the U6 promoter-driven site of the same vector, replacing the non-targeting sequence. Lentiviral particles were produced by co-transfecting HEK293T cells with the expression or knockdown plasmid together with packaging plasmids (psPAX2 and pMD2.G) using Lipofectamine 3000 (Thermo Fisher Scientific, L3000008). Viral supernatants were collected 48 h post-transfection and used to infect OV-90 and OVCAR3 cells. Stable cell lines were selected with puromycin (1 μg/mL) for one week.

CCK-8 and the EdU assays

Cell proliferation was assessed using the CCK-8 assay and the EdU assay. For CCK-8, cells were seeded in 96-well plates at a density of 2×10^3 cells/well. At indicated time points, 10 μL of CCK-8 reagent (Beyotime, C0046) was added to each well, incubated for 2 h at 37°C, and absorbance was measured at 450 nm. For EdU assay, cells were cultured in 96-well plates and treated with EdU (Beyotime, C0072L) for 2 h, followed by fixation and staining according to the manufacturer's protocol. Images were captured using a fluorescence microscope, and the percentage of EdU-positive cells was quantified.

Wound-healing and Transwell migration assays

Cell migratory capacity was evaluated by wound-healing assay and Transwell migration assay. For wound healing, cells were seeded in 6-well plates and grown to confluence. A linear scratch was made using a sterile 200 μL pipette tip, and detached cells were removed by PBS washes. Cells were then cultured in medium containing 2% FBS, and wound closure was observed and photographed at 0 and 36 h. The migration distance was measured using ImageJ software. For Transwell assay, 5×10^4 cells suspended in serum-free medium were seeded into the upper chamber of Transwell inserts (8 μm pore size). Medium containing 10% FBS was added to the lower chamber. After 24 h incubation, non-migrated cells on the upper membrane surface were removed with a cotton swab, and migrated cells were fixed with 4% paraformaldehyde, stained with 0.1% crystal violet, and counted under a microscope in five random fields.

TUNEL assay

Apoptosis was detected by TUNEL. OV-90 and OVCAR3 cells were seeded on sterile coverslips placed in 24-well plates at a density of 5×10^4 cells per well and cultured overnight for attachment. Cells were then exposed to stress conditions induced by treatment with 10 μM cisplatin for 24 h to trigger apoptosis. Following treatment, cells were fixed with 4% paraformaldehyde for 20 min at room temperature and permeabilized with 0.1% Triton X-100 in PBS for 5 min. TUNEL staining was performed using the One Step TUNEL Apoptosis Assay Kit (Beyotime, C1098) according to the manufacturer's instructions. Nuclei were counterstained with DAPI. Coverslips were mounted onto glass slides and imaged under a fluorescence microscope. The percentage of TUNEL-positive cells was quantified in at least five randomly selected fields per sample using ImageJ software.

In vivo tumorigenesis assay

Four-week-old female BALB/c nude mice were obtained and maintained under specific pathogen-free conditions (Animal Facility of Shanghai Institute of Cell Biology, Chinese Academy of Sciences, Shanghai, China). OV-90 cells (5×10^6) stably overexpressing CAAP1, knockdown CAAP1, or control vector were resuspended in 100 μL PBS and subcutaneously injected into the dorsolateral flank of each mouse. Tumor dimensions were measured every two days with vernier caliper, and tumor volume was calculated using the formula: volume = 0.52 × length × width^2. On day 21 post-inoculation, mice were humanely euthanized by gradual carbon dioxide (CO_2) inhalation in a sealed chamber. The CO_2 displacement rate was adjusted to 20% to 30% of the chamber volume per minute to ensure rapid, stress-free loss of consciousness. After the cessation of spontaneous respiration was visually confirmed, the mice were maintained in the CO_2-enriched atmosphere for an additional 3-5 minutes to guarantee complete and irreversible death. Euthanasia was definitively confirmed by the absence of a palpable heartbeat and respiratory movements prior to necropsy. Subsequently, tumors were excised, weighed, and processed for Ki67 immunofluorescence staining. All animal procedures were approved by the Institutional Animal Care and Use Committee of the First People's Hospital of JiangsuAnipheBiolaboratoryInc (LYDY-A-20250901191, September 1, 2025).

LC-MS/MS

Whole-cell lysates from OV-90 cells were subjected to immunoprecipitation with an anti-CAAP1 antibody or control IgG. The immunoprecipitated complexes were resolved by SDS-PAGE, and protein bands were excised and digested with trypsin. The resulting peptides were analyzed by LC-MS/MS. Candidate interacting proteins were identified by searching the spectra against the human UniProt database.

Co-IP and Western blot

For endogenous Co-IP, whole-cell lysates from OV-90 and OVCAR3 cells were prepared using IP lysis buffer supplemented with protease inhibitors. Lysates were incubated with anti-CAAP1 antibody or normal rabbit IgG overnight at 4°C, followed by incubation with protein A/G magnetic beads for an additional 2 h. The immunocomplexes were washed extensively, eluted with SDS sample buffer, and subjected to immunoblotting with anti-EIF3I antibody to detect the endogenous interaction. For exogenous Co-IP, 293T cells were co-transfected with FLAG-tagged EIF3I and His-tagged CAAP1 expression plasmids using Lipofectamine 3000. At 48 h post-transfection, cells were harvested and lysed. Cell lysates were incubated with anti-FLAG affinity gel or control IgG overnight at 4°C. After washing, bound proteins were eluted and analyzed by Western blot using anti-His antibody to confirm the reciprocal interaction between CAAP1 and EIF3I.

For Western blot, equal amounts of protein were separated by SDS-PAGE, transferred to PVDF membranes, blocked with 5% non-fat milk, and incubated with primary antibodies overnight at 4°C, followed by HRP-conjugated secondary antibodies. Protein bands were visualized using an enhanced chemiluminescence system.

Statistical analysis

All experiments were performed independently at least three times, and data are presented as the mean ± standard deviation (SD). Statistical analyses were carried out using GraphPad Prism 8.0. Comparisons between two groups were conducted using unpaired two-tailed Student's t-test, and comparisons among multiple groups were analyzed by one-way ANOVA followed by Tukey's post hoc test for pairwise multiple comparisons. For comparisons involving multiple groups over time, repeated-measures two-way ANOVA was applied. When the interaction effect was significant, Bonferroni's post hoc test was performed for multiple comparisons at each time point. Survival curves were generated using the Kaplan-Meier method and compared by log-rank test. A *P*-value < 0.05 was considered statistically significant (*P < 0.05, **P < 0.01, ***P < 0.001, ****P < 0.0001).

Results

CAAP1 downregulation predicts poor prognosis in HGSOC

We obtained RNA sequencing data of 204 serous ovarian carcinoma (SOC) samples from

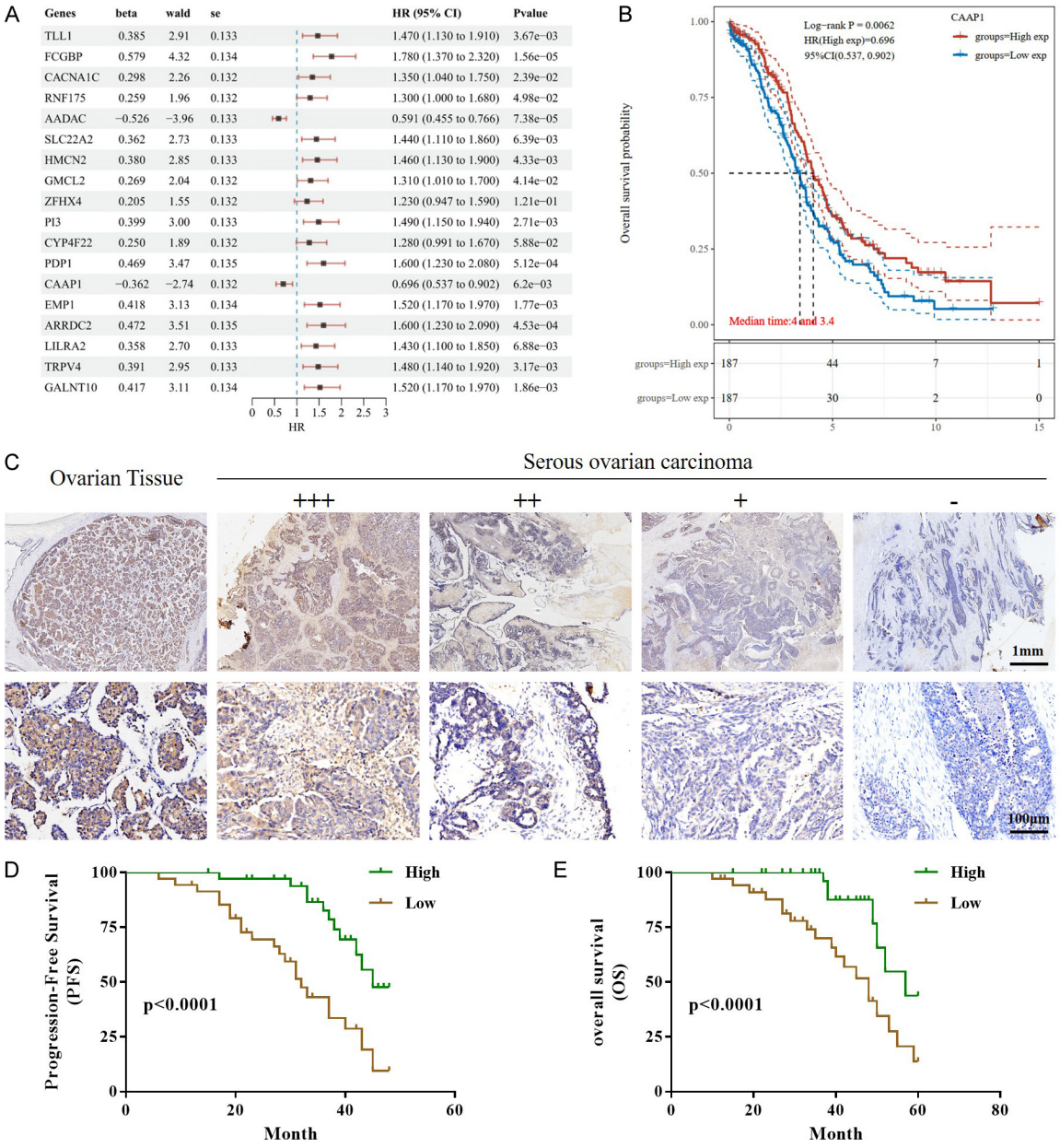

Figure 1. CAAP1 downregulation predicts poor prognosis in HGSOC. (A) List of the top 18 genes most significantly associated with overall survival in SOC identified by genome-wide univariate Cox regression analysis of TCGA RNAseq data. (B) Kaplan-Meier curves for overall survival in the SOC cohort stratified by median expression level of CAAP1. (C) Representative immunohistochemical staining of CAAP1 in paired HGSOC tumor tissues and adjacent normal ovarian tissues on tissue microarray. (D, E) Kaplan-Meier analysis of PFS (D) and OS (E) in the HGSOC patient cohort stratified by IHC score of CAAP1. Statistical significance was determined by the log-rank test. Scale bars, 1 mm and 100 μm.

the TCGA database (https://portal.gdc.cancer.gov). Through genome-wide univariate Cox regression analysis, we identified 18 genes that were most significantly associated with prognosis (**Figure 1A**). Using the median expression level of each gene as the cut-off for grouping, survival analysis revealed that CAAP1 expression was positively correlated with SOC prognosis (**Figure 1B**). Considering that RNA levels may not entirely reflect protein expression, we subsequently performed immunohistochemistry (IHC) for CAAP1 on a tissue micro-

array containing paired samples from 71 cases of HGSOC and adjacent normal tissue. Results showed that CAAP1 expression was lower in tumor tissues compared to adjacent normal tissues (**Figure 1C**). Clinicopathological correlation analysis further demonstrated that the expression level of CAAP1 was significantly positively correlated with both progression-free survival (PFS) rate and overall survival (OS) rate in HGSOC patients (**Figure 1D**, **1E**).

CAAP1 downregulation promotes cell proliferation in HGSOC

We performed Western blot analysis on 18 pairs of HGSOC clinical samples, and the results demonstrated that the expression level of CAAP1 in tumor tissues was significantly lower than that in corresponding adjacent normal tissues (**Figure 2A**). Consistent with this, at the cellular level, compared with the normal ovarian epithelial cell line IOSE-80, CAAP1 was downregulated to varying degrees in multiple HGSOC cell lines (OVAR79, OVPA8, OV-90, OVCAR3), the low-grade serous ovarian cancer (LGSOC) cell line HO-8910, and the cell line SKOV3 of controversial origin (**Figure 2B**). Given that HGSOC is the most common and aggressive subtype of OC, we further investigated the effect of CAAP1 on HGSOC cells proliferation. Thus, we established stable CAAP1-overexpressing and stable CAAP1-knockdown cell models via lentiviral transfection in OV-90 and OVCAR3 cell lines, and validated by Western blot (**Figure 2C**, **2D**). Functional assays demonstrated that CAAP1 knockdown promoted OV-90 and OVCAR3 cells proliferation, whereas overexpressing CAAP1 inhibited their proliferative activity. This conclusion was verified by both CCK-8 assays (**Figure 2E**, **2F**) and EdU assays (**Figure 2G**).

CAAP1 downregulation enhances cell migration and apoptosis resistance in HGSOC

To elucidate the direct role of CAAP1 in metastasis, we examined the capacity of cellular migratory in HGSOC cells with CAAP1 overexpress or knockdown. Wound-healing assays and Transwell migration assays were performed to quantitatively assess cell migration. The results consistently showed that CAAP1 knockdown significantly enhanced the migratory capacity of both OV-90 and OVCAR3 cells, as evidenced by accelerated wound closure and increased numbers of migrated cells (**Figure 3A**, **3B**). Conversely, CAAP1 overexpression exerted an inhibitory effect on cell migration. In addition to migration, we investigated the effect of CAAP1 on apoptosis resistance. TUNEL assay revealed that CAAP1-knockdown HGSOC cells exhibited a markedly reduced rate of apoptosis under stress conditions, indicating a substantial enhancement in their ability to resist programmed cell death (**Figure 3C**). Collectively, these data demonstrate that CAAP1 downregulation effectively promotes two critical malignant phenotypes in HGSOC, the enhanced migratory potential and increased resistance to apoptosis.

CAAP1 overexpression inhibites HGSOC growth in vivo

To further explore the biological functions of CAAP1 in vivo, we subcutaneously implanted OV-90 cells with stable CAAP1 knockdown or overexpression, along with control cells, into the dorsolateral region of the flank of BALB/c nude mice. Beginning on day 7 post-inoculation, the longest and shortest diameters of the tumors were measured every two days using a caliper, and the tumor volume was calculated accordingly. On day 21 after inoculation, all mice were euthanized, the subcutaneous xenograft tumors were completely excised and weighed. The results demonstrated that compared with the control group, tumor growth was significantly accelerated in CAAP1 knockdown group, while tumor growth was markedly suppressed in CAAP1 overexpression group (**Figure 4A**). Ki67 immunofluorescence analysis of xenograft tumors revealed that the proportion of Ki67-positive cells was significantly higher in CAAP1 knockdown group. In contrast, the Ki67-positive rates remained relatively low in both the control group and the CAAP1 overexpression group (**Figure 4B**). Collectively, these in vivo experimental data confirm that CAAP1 deficiency exerts a clear protumorigenic effect at the animal level, which is consistent with the findings from the aforementioned cellular-level studies.

EIF3I is identified as the CAAP1-interacting protein

As described above, the loss of CAAP1 expression plays a crucial role in the HGSOC progression. To further explore the molecular mecha-

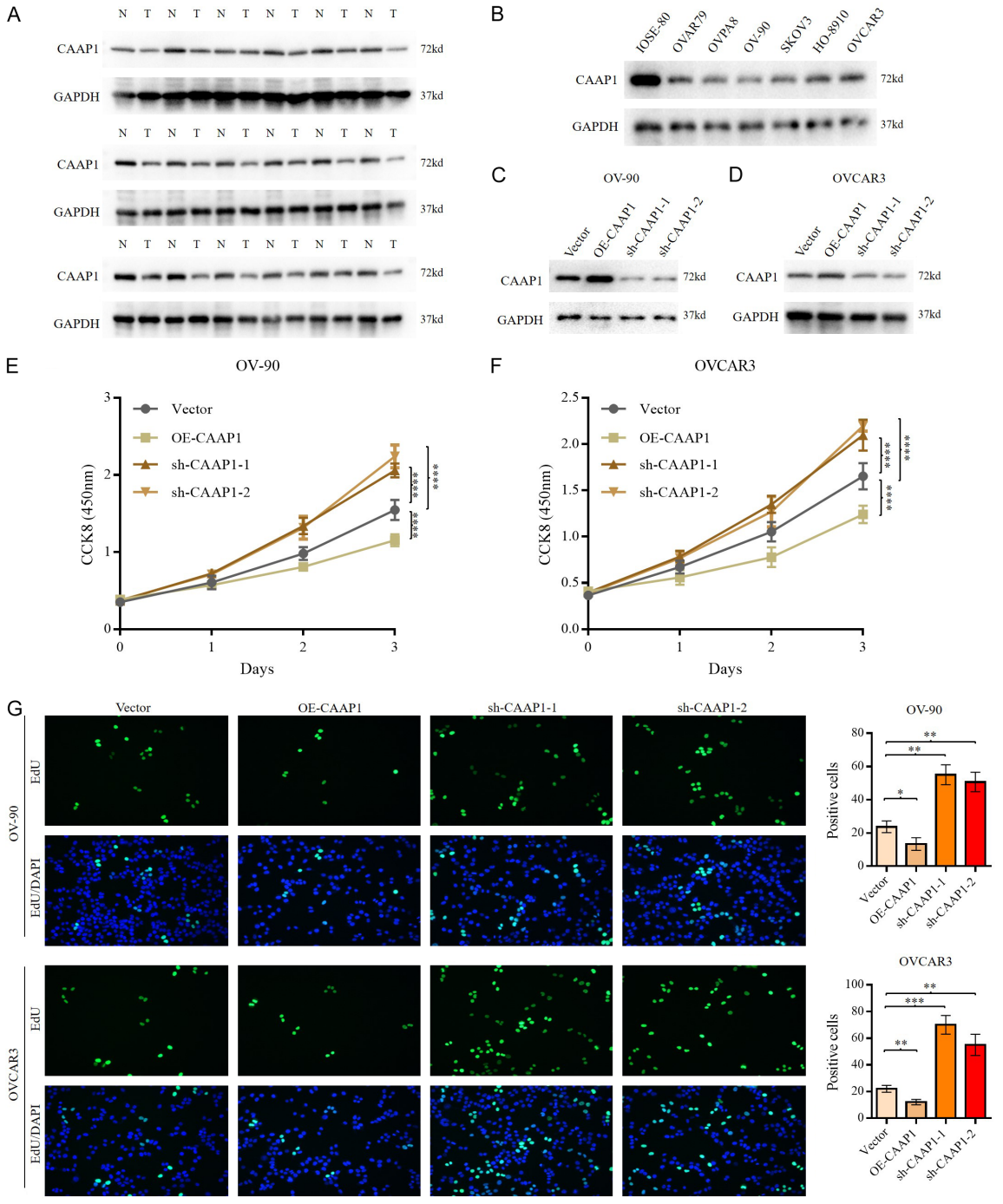

Figure 2. CAAP1 downregulation promotes cell proliferation in HGSOC. (A) Western blot analysis of CAAP1 protein expression in 18 pairs of HGSOC tumor tissues (T) and adjacent normal ovarian tissues (N). (B) Basal levels of CAAP1 protein in normal ovarian epithelial cell line IOSE80, LGSOC cell line HO8910, ovarian adenocarcinoma cell line SKOV3, and HGSOC cell lines OV90 and OVCAR3. (C, D) Validation of CAAP1 overexpression and knockdown efficiency in OV90 (C) and OVCAR3 (D) cells by Western blot. (E, F) Assessment of proliferation following CAAP1 overexpression or knockdown in OV90 (E) and OVCAR3 (F) cells using the CCK-8 assay. Absorbance at 450 nm was measured daily for four consecutive days. (G) Representative fluorescence images and quantification of EdU incorporation assay in OV90 and OVCAR3 cells. EdU-positive cells (green) represent proliferating cells; nuclei were counterstained with DAPI (blue). Experiments were repeated three times with different cell batches on separate days. Quantification data are presented as mean ± SD from three independent biological replicates (n = 3). For CCK-8 time-course data, statistical analysis was performed using repeated-measures two-way ANOVA followed by Bonferroni's post hoc test for comparisons at individual time points. For EdU quantification, one-way ANOVA followed by Tukey's post hoc test for pairwise multiple comparisons was used. ****P < 0.0001. Scale bar, 100 μm.

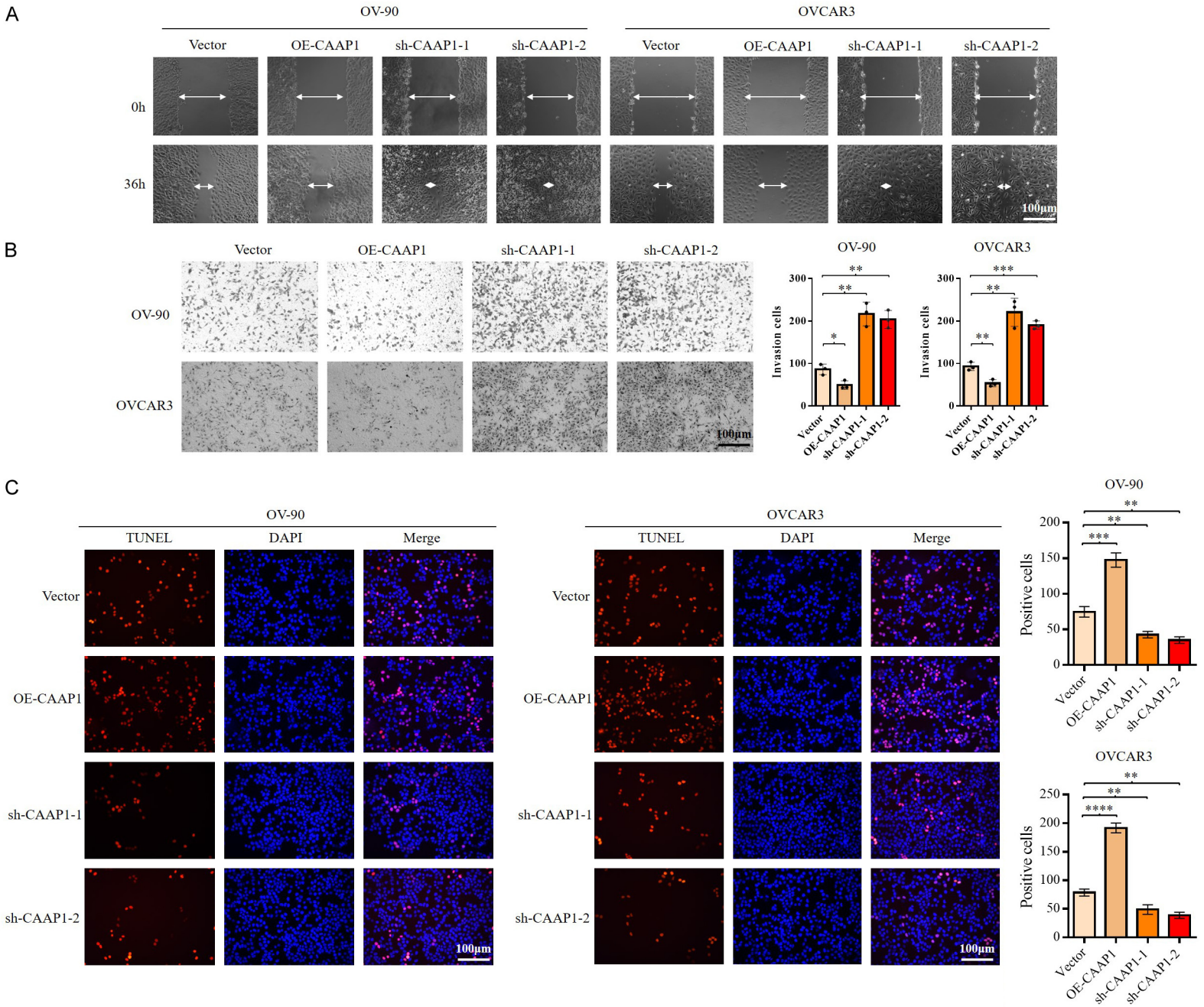
A
OV-90
OVCAR3
Vector
OE-CAAP1
sh-CAAP1-1
sh-CAAP1-2
0h
36h
100μm
B
OV-90
OVCAR3
Invasion cells
C
TUNEL
DAPI
Merge
Positive cells
****

Figure 3. CAAP1 downregulation enhances cell migration and apoptosis resistance in HGSOC. A. Representative images and quantification of wound-healing assay in OV-90 and OVCAR3 cells with CAAP1 overexpression or knockdown. Wound closure was monitored at 0 and 36 h. B. Representative images and quantification of Transwell migration assay. C. TUNEL assay assessing apoptosis in OV-90 and OVCAR3 cells treated with 10 μM cisplatin for 24 h. TUNEL-positive nuclei (red) indicate apoptotic cells; nuclei were counterstained with DAPI (blue). Experiments were repeated three times with different cell batches on separate days. Quantification data are presented as mean ± SD from three independent biological replicates (n = 3). Statistical analysis was performed by one-way ANOVA followed by Tukey's post hoc test. *P < 0.05, *P < 0.01, ***P < 0.001. Scale bar, 100 μm.

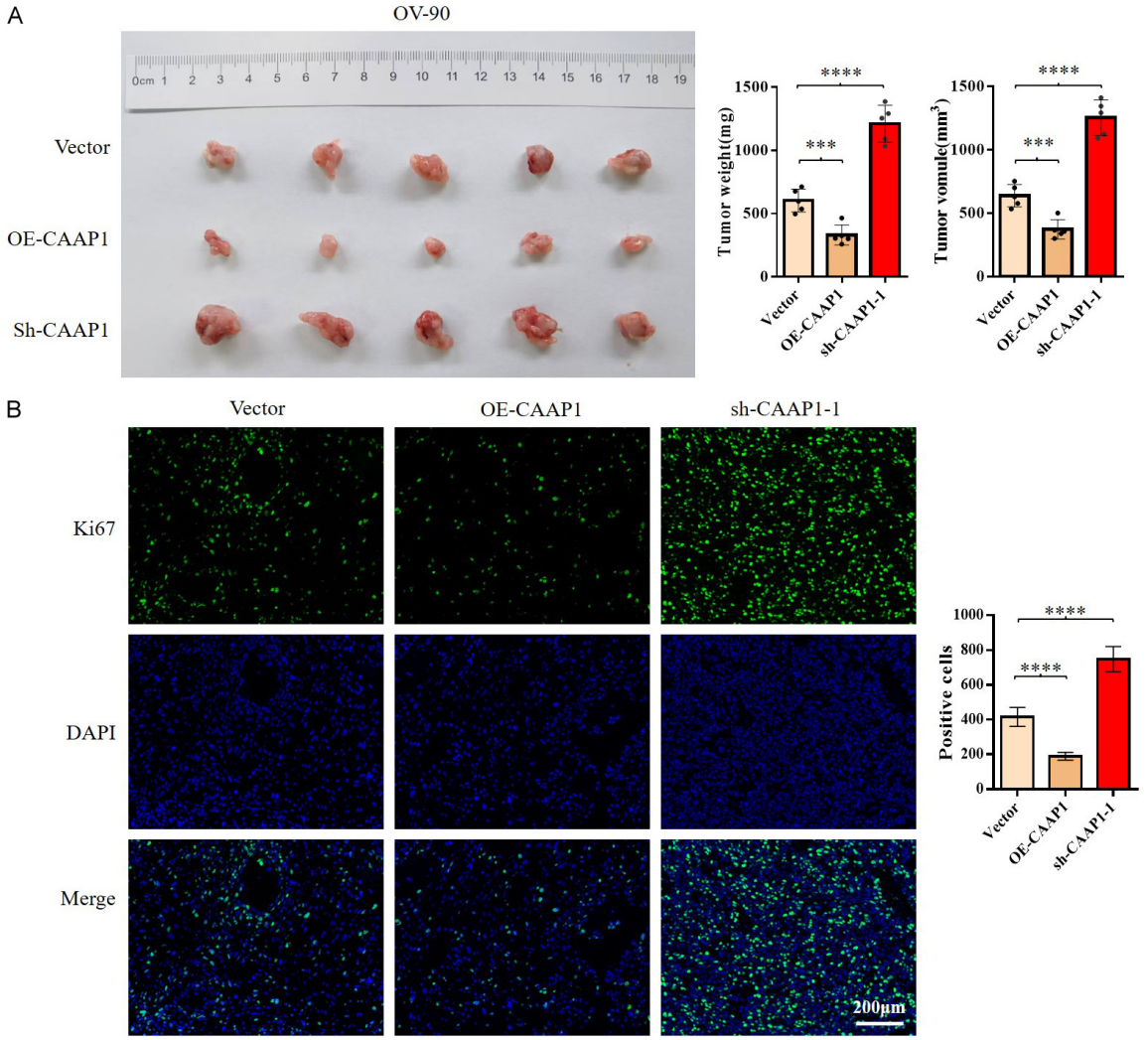

Figure 4. CAAP1 overexpression inhibites HGSOC growth in vivo. A. Representative images of subcutaneous xenograft tumors and quantitative data on tumor weight and volume. Tumors were harvested from BALB/c nude mice 21 days after inoculation with wild-type or CAAP1 stably over-expressing/knockdown OV90 cells. B. Representative immunofluorescence staining of Ki67 (green) in xenograft tumor sections; nuclei were counterstained with DAPI (blue). Experiments were repeated three times with different cell batches on separate days. Quantification data are presented as mean ± SD from three independent biological replicates (n = 3). For tumor volume, statistical analysis was performed using repeated-measures two-way ANOVA followed by Bonferroni's post hoc test for comparisons at individual time points; for tumor weights and Ki67-positive rates, one-way ANOVA followed by Tukey's post hoc test was used. ***P < 0.001, ****P < 0.0001. Scale bar, 200 μm.

nism, we first performed LC-MS/MS analysis to identify potential proteins that may interact with CAAP1 (**Figure 5A**). LC-MS/MS analysis identified EIF3I as a target specifically interacting with CAAP1 (**Figure 5B**). Subsequently, we conducted immunoprecipitation in OV-90 and

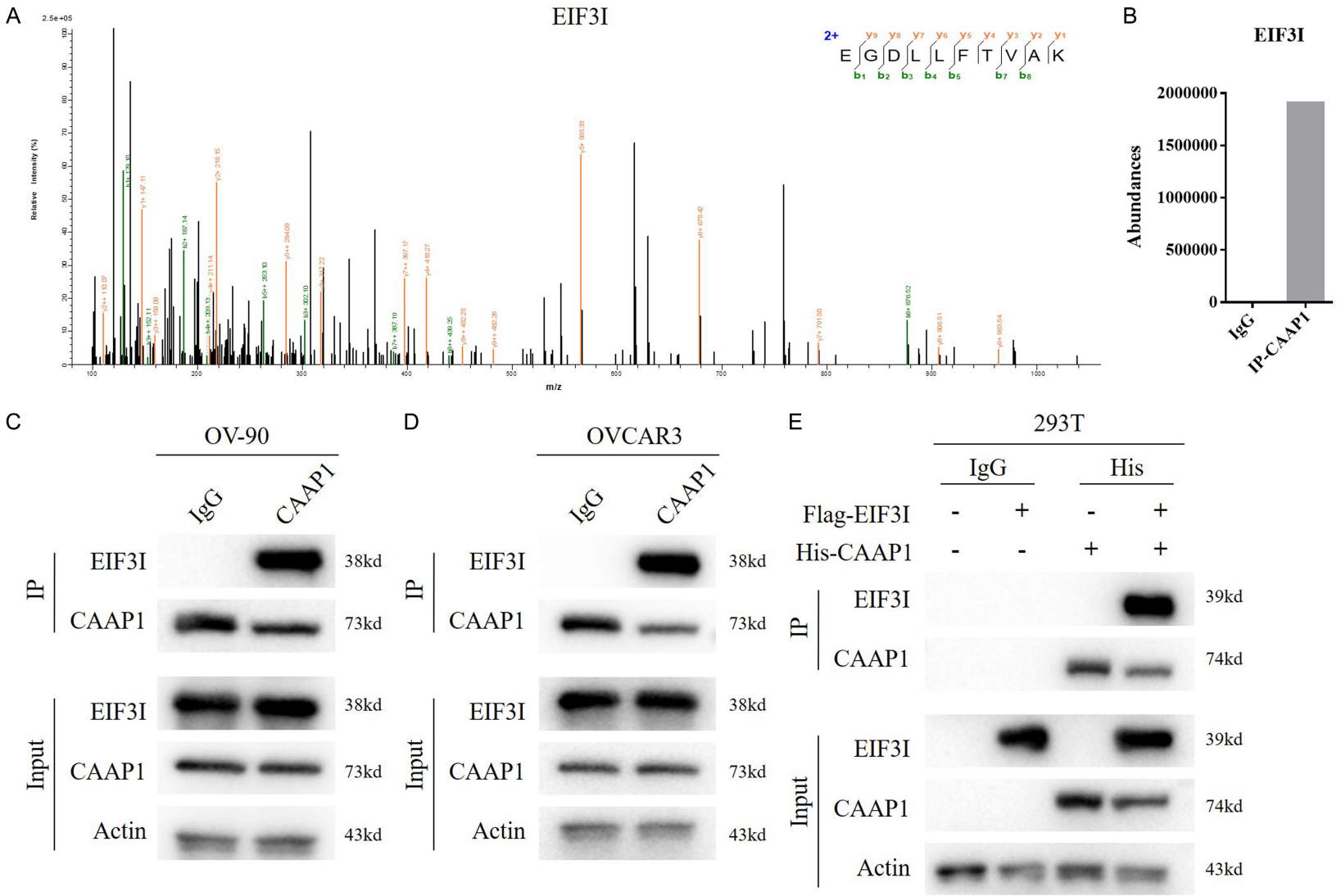

Figure 5. EIF3I is identified as the CAAP1-interacting protein. A. Coomassie Blue-stained SDS-PAGE gel of immunoprecipitates from OV-90 whole-cell lysates using anti-CAAP1 antibody or control IgG. A specific band corresponding to the expected molecular weight of EIF3I was excised and subjected to LC-MS/MS analysis. B. Representative tandem mass spectrometry (MS/MS) spectrum of a tryptic peptide derived from EIF3I (sequence coverage shown). C, D. Endogenous Co-IP assay in OV-90 and OVCAR3 cells. E. FLAG-tagged EIF3I and His-tagged CAAP1 expression plasmids were co-transfected into HEK293T cells for exogenous reciprocal Co-IP validation.

OVCAR3 cells. When CAAP1 was immunoprecipitated using protein A/G magnetic beads and analyzed by immunoblotting with the specified antibodies, the EIF3I protein was detected in both OV-90 and OVCAR3 cell lines (**Figure 5C**, **5D**). Furthermore, FLAG-tagged EIF3I and His-tagged CAAP1 were co-transfected into 293T cells, and the interaction between exogenous CAAP1 and EIF3I was assessed by immunoprecipitation. The results showed that FLAG was detected upon His pull-down, indicating an interaction between CAAP1 and EIF3I (**Figure 5E**).

CAAP1-EIF3I interaction regulates proliferation- and migration proteins

Previous studies have shown that in papillary thyroid carcinoma, circEIF3I interacts with the RNA-binding protein AUF1, reducing Cyclin D1 mRNA degradation and promoting tumor progression [14]. In colorectal cancer, EIF3I facilitates migration/invasion by regulating the epithelial-mesenchymal transition (EMT) process [15]. Furthermore, overexpression of the single subunit of the eukaryotic translation initiation factor EIF3 in mammalian cells can confer oncogenic properties, including enhanced proliferative and growth capacity as well as increased global protein synthesis rates [16]. To investigate the biological effects resulting from the interaction between CAAP1 and EIF3I, we either overexpressed or knocked down CAAP1 in OV-90 and OVCAR3 cells and examined changes in the expression of Cyclin D1, c-Myc, and EMT-related markers. Results showed that CAAP1 knockdown upregulates the expression of Cyclin D1, c-Myc, and the mesenchymal markers N-cadherin and vimentin, while downregulating the expression of the epithelial marker E-cadherin (**Figure 6A**, **6B**). These findings demonstrate that in HGSOC, CAAP1 interacted with EIF3I to regulate the expression of key oncogenic proteins, including Cyclin D1, c-Myc, and EMT-related molecules, thereby exerts tumor-suppressive role.

To further validate that EIF3I serves as a key downstream effector of CAAP1, we knocked down EIF3I in OV-90 and OVCAR3 cells (**Figure 6C**, **6D**) and detected the expression of downstream proteins (Cyclin D1, c-Myc, E-cadherin, N-cadherin, and Vimentin) by Western blotting. The results showed that, compared with CAAP1 knockdown alone, simultaneous knockdown of both CAAP1 and EIF3I led to completely opposite expression trends of these proteins (**Figure 6E**, **6F**), indicating that EIF3I depletion effectively abrogated the downstream signaling alterations induced by CAAP1 downregulation. These findings suggest that EIF3I is essential for CAAP1 to exert its functional role.

Discussion

HGSOC is the gynecological malignancy with the highest mortality rate. Most patients present with extensive peritoneal metastasis at initial diagnosis, and the disease is prone to recurrence and drug resistance following treatment. Although surgery combined with chemotherapy is the standard treatment, the molecular mechanisms driving metastasis remain understood, hindering the development of effective therapies. Therefore, elucidating the regulatory mechanisms of HGSOC metastasis and colonization at secondary sites, particularly identifying key regulatory factors, is crucial for improving patient outcomes. This study systematically reveals the tumor-suppressive function of CAAP1 in HGSOC. Notably, CAAP1 has been widely reported as an oncogenic factor in cancers such as colorectal cancer and hepatoma, where it drives tumor progression by inhibiting apoptosis and promoting proliferation and migration. This contradiction suggests that the function of CAAP1 exhibits significant 'context-dependency', with its biological effects may dependent on tissue origin, molecular background, and tumor microenvironment. Our findings not only expand the understanding of CAAP1 functional diversity but also emphasize the importance of conducting independent mechanistic investigations in specific cancer types, avoiding the oversimplified extrapolation of conclusions drawn from other malignancies.

Mechanistically, we identified EIF3I as a key CAAP1-interacting protein in HGSOC through proteomic interaction analysis. As an integral component of the multi-subunit eIF3 complex, EIF3I plays a pivotal role in protein translation initiation [17]. Accumulating evidence has demonstrated that eIF3 subunits dysregulation drives tumorigenesis, metastasis, and drug resistance by selectively modulating specific mRNAs translation [18, 19]. For instance, EIF3I has been shown to promote invasion via regu-

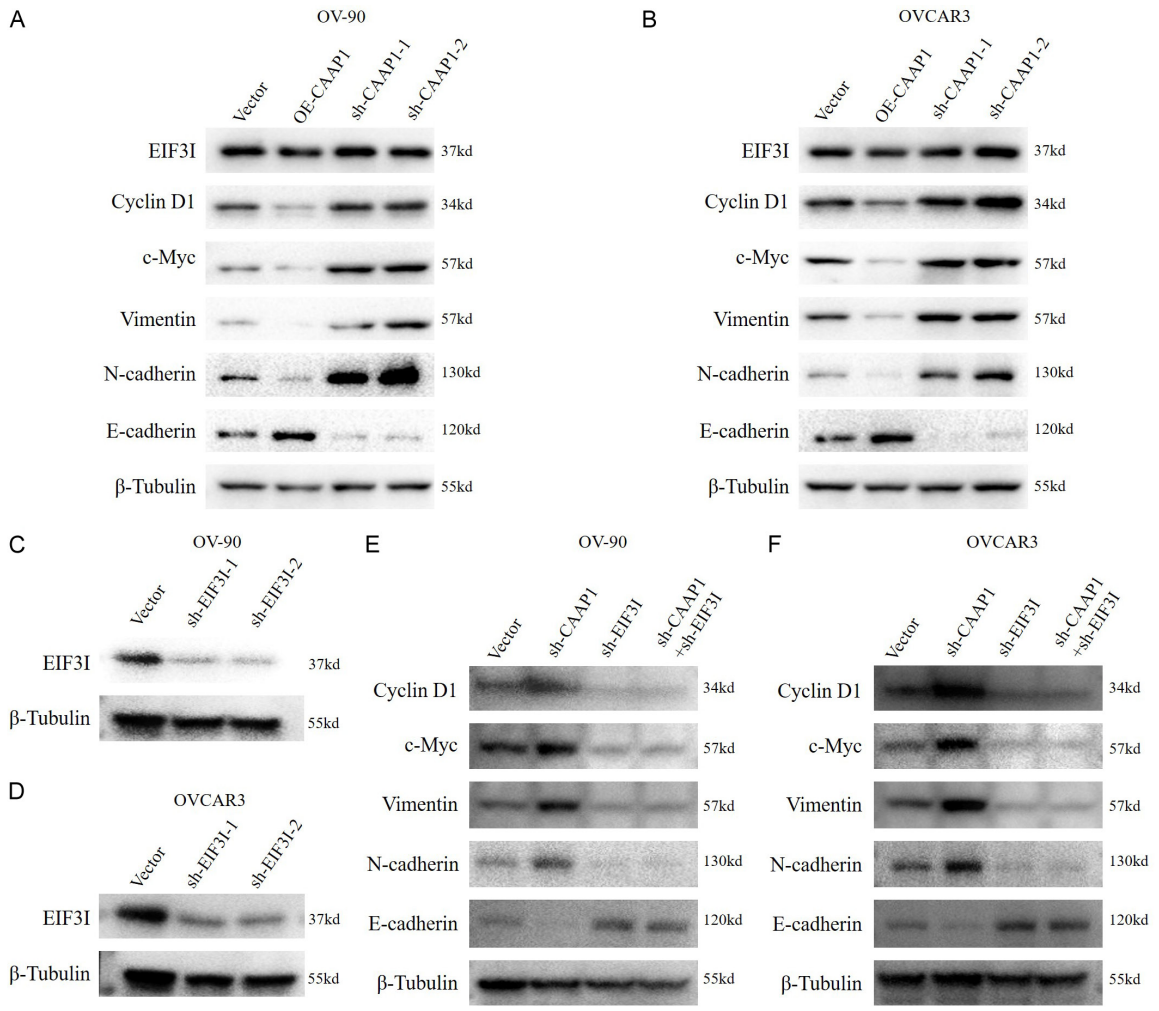

Figure 6. CAAP1-EIF3I interaction regulates proliferation- and migration proteins. (A, B) Western blot analysis of EIF3I, Cyclin D1, cMyc, and epithelial-mesenchymal transition (EMT) markers (E-cadherin, N-cadherin, vimentin) expression in OV90 (A) and OVCAR3 (B) cells with stable overexpression/knockdown of CAAP1 or vector control. (C, D) Western blot confirmed the knockdown efficiency of EIF3I in OV-90 (C) and OVCAR3 (D) cells. (E, F) Western blot analysis of Cyclin D1, c-Myc, and EMT markers (E-cadherin, N-cadherin, and vimentin) protein expression levels in OV-90 (E) and OVCAR3 (F) cells following single knockdown of CAAP1, single knockdown of EIF3I, or simultaneous knockdown of both CAAP1 and EIF3I.

lating epithelial-mesenchymal transition (EMT) in colorectal cancer [15]. In hepatocellular carcinoma, EIF3I promotes angiogenesis through regulating VEGF synthesis [20]. Building on these findings, our study further suggests that under normal conditions, CAAP1, through its regulation of EIF3I, may interfere with the interaction between EIF3I and its target mRNAs or other subunits of the translation initiation complex, thereby selectively suppressing EIF3I-mediated translation initiation. However, in HGSOC, CAAP1 is aberrantly downregulated, which attenuates its inhibitory effect on EIF3I and consequently enhances EIF3I function. This enhanced EIF3I activity upregulates the translational efficiency of proliferation-associated proteins (Cyclin D1, c-Myc) and EMT-related proteins (N-cadherin, Vimentin), ultimately promoting HGSOC cell proliferation and migration.

The findings of this study hold potential clinical translational value. First, CAAP1 expression levels are significantly correlated strongly with HGSOC patients survival, suggesting its utility as a complementary prognostic biomarker for identifying patients at high recurrence risk and guiding individualized clinical management.

Second, and more importantly, the identification of CAAP1-EIF3I interaction reveals a novel potential therapeutic targets. Given the inherent challenges in directly restoring or delivering tumor suppressors, a viable strategy lies in developing small-molecule inhibitors or peptide-based therapeutics that mimic CAAP1 function to specifically disrupt the oncogenic activity of EIF3I. Furthermore, exploring compounds that stabilize CAAP1 protein or upregulate its expression represents a promising therapeutic direction worthy of investigation.

Nevertheless, this study has several limitations that also suggest directions for future research. First, while we have demonstrated the interaction between CAAP1 and EIF3I and its impact on downstream protein expression, the precise mechanism by which CAAP1 modulates EIF3I activity requires further elucidation. Second, the subcutaneous xenograft model primarily used in this study, although sufficient to demonstrate the inhibitory effect of CAAP1 on tumor growth, does not fully recapitulate the complete metastatic cascade of HGSOC, which involves detachment, suspension, reattachment, and colonization within the peritoneal cavity. Future studies employing orthotopic transplantation or peritoneal dissemination models will enable a more accurate assessment of the role of CAAP1 in suppressing metastatic colonization, the most critical step in this process. Finally, the epigenetic or transcriptional mechanisms underlying CAAP1 downregulation in HGSOC remain unclear; exploring its upstream regulatory factors will be essential for a comprehensive understanding of the dysregulation of this pathway.

Conclusion

Collectively, the present study establishes CAAP1 as a novel tumor suppressor in HGSOC through multi-level evidence. CAAP1 downregulation correlates with poor patient prognosis and functionally promotes tumor progression by enhancing proliferation, migration, and resistance to apoptosis. Mechanistically, CAAP1 negatively regulates the expression of Cyclin D1, c-Myc, and EMT-associated proteins through interaction with the translation initia tion factor EIF3I. These findings not only provide new insights into the mechanisms underlying metastasis and malignant proliferation in HGSOC but also lay a theoretical foundation for the development of prognostic assessment tools and potential therapeutic strategies targeting CAAP1-EIF3I axis.

Disclosure of conflict of interest

None.

Address correspondence to: Dr. Weiwei Qian, Department of Gynecology, The Affiliated Lianyungang Hospital of Xuzhou Medical University/The First People's Hospital of Lianyungang, No. 6, Zhenhua East Road, Lianyungang 222000, Jiangsu, China. E-mail: qianweiweilyg@njmu.edu.cn; Dr. Chunlei Zhang, Department of Orthopedics, Nanjing Hospital of Chinese Medicine Affiliated to Nanjing University of Chinese Medicine, No. 157, Daming Road, Nanjing 210000, Jiangsu, China. E-mail: chunleizh@126.com

References

[1] Xu J, Fang Y, Chen K, Li S, Tang S, Ren Y, Cen Y, Fei W, Zhang B, Shen Y and Lu W. Single-cell RNA sequencing reveals the tissue architecture in human high-grade serous ovarian cancer. Clin Cancer Res 2022; 28: 3590-3602.

[2] Seidman JD, Horkayne-Szakaly I, Haiba M, Boice CR, Kurman RJ and Ronnett BM. The histologic type and stage distribution of ovarian carcinomas of surface epithelial origin. Int J Gynecol Pathol 2004; 23: 41-44.

[3] Bowtell DD, Böhm S, Ahmed AA, Aspuria PJ, Bast RC Jr, Beral V, Berek JS, Birrer MJ, Blagden S, Bookman MA, Brenton JD, Chiappinelli KB, Martins FC, Coukos G, Drapkin R, Edmondson R, Fotopoulou C, Gabra H, Galon J, Gourley C, Heong V, Huntsman DG, Iwanicki M, Karlan BY, Kaye A, Lengyel E, Levine DA, Lu KH, Mcneish IA, Menon U, Narod SA, Nelson BH, Nephew KP, Pharoah P, Powell DJ Jr, Ramos P, Romero IL, Scott CL, Sood AK, Stronach EA and Balkwill FR. Rethinking ovarian cancer II: reducing mortality from high-grade serous ovarian cancer. Nat Rev Cancer 2015; 15: 668-679.

[4] Lupia M, Melocchi V, Bizzaro F, Lo Riso P, Dama E, Baronio M, Ranghiero A, Barberis M, Bernard L, Bertalot G, Giavazzi R, Testa G, Bianchi F and Cavallaro U. Integrated molecular profiling of patient-derived ovarian cancer models identifies clinically relevant signatures and tumor vulnerabilities. Int J Cancer 2022; 151: 240-254.

[5] Micek HM, Rosenstock L, Ma Y, Hielsberg C, Montemorano L, Gari MK, Ponik SM and Kreeger PK. Model of collective detachment

in high-grade serous ovarian cancer demonstrates that tumor spheroids produce ECM to support metastatic processes. APL Bioeng 2023; 7: 16111.
[6] Sawyer BT, Qamar L, Yamamoto TM, Mcmellen A, Watson ZL, Richer JK, Behbakht K, Schlaepfer IR and Bitler BG. Targeting fatty acid oxidation to promote anoikis and inhibit ovarian cancer progression. Mol Cancer Res 2020; 18: 1088-1098.
[7] Hardy LR, Pergande MR, Esparza K, Heath KN, Önyüksel H, Cologna SM and Burdette JE. Proteomic analysis reveals a role for PAX8 in peritoneal colonization of high grade serous ovarian cancer that can be targeted with micelle encapsulated thiostrepton. Oncogene 2019; 38: 6003-6016.
[8] Zhang HM, Li H, Wang GX, Wang J, Xiang Y, Huang Y, Shen C, Dai ZT, Li JP, Zhang TC and Liao XH. MKL1/mir-5100/CAAP1 loop regulates autophagy and apoptosis in gastric cancer cells. Neoplasia 2020; 22: 220-230.
[9] Su JH, Lu HJ, Wang YT, Kong YX, Liu YT, Wang MM, Xiong YN and Zhang GL. Effects of CAAP1 on proliferation, migration and invasion of hepatoma cell line SMMC-7721. Sichuan Da Xue Xue Bao Yi Xue Ban 2021; 52: 445-451.
[10] Aslam MA, Alemdehy MF, Pritchard CEJ, Song JY, Muhaimin FI, Wijdeven RH, Huijbers IJ, Neefjes J and Jacobs H. Towards an understanding of c9orf82 protein/CAAP1 function. PLoS One 2019; 14: e0210526.
[11] Wijdeven RH, Pang B, van der Zanden SY, Qiao X, Blomen V, Hoogstraat M, Lips EH, Janssen L, Wessels L, Brummelkamp TR and Neefjes J. Genome-wide identification and characterization of novel factors conferring resistance to topoisomerase II poisons in cancer. Cancer Res 2015; 75: 4176-4187.
[12] Zhang KX, Ding C, Liu QH and Zhu DM. Knockdown of LINC01087 inhibits gastric cancer malignant behavior by regulating the mir-135a-5p/CAAP1 axis. Funct Integr Genomics 2023; 23: 248.
[13] Ni M, Zhou J, Gong W, Jiang R, Li X, Dai W, Yin Z, Chen Z, Zheng Z and Zhu J. Proteomic analysis reveals CAAP1 negatively correlates with platinum resistance in ovarian cancer. J Proteomics 2023; 277: 104864.
[14] Yao X, Liu H, Wang Z, Lu F, Chen W, Feng Q, Miao Y, Zhang J, Wang Y, Chen Y, Xue L, Liu Y, Chen L and Zhang Q. Circular RNA EIF3i promotes papillary thyroid cancer progression by interacting with AUF1 to increase cyclin d1 production. Oncogene 2023; 42: 3206-3218.
[15] Huang Q, Zhao J, Zhang Y, Zhou Y, Yang X, Chen X, Wei M, Han J and Zhang Y. EIF3i facilitates NELFCD translation to promote metastasis via regulating EMT and invadopodia. Br J Cancer 2026; 134: 996-1005.
[16] Roobol A, Roobol J, Smith ME, Carden MJ, Hershey JWB, Willis AE and Smales CM. Engineered transient and stable overexpression of translation factors eIF3i and eIF3c in CHOK1 and HEK293 cells gives enhanced cell growth associated with increased c-myc expression and increased recombinant protein synthesis. Metab Eng 2020; 59: 98-105.
[17] Ma S, Dong Z, Cui Q, Liu J and Zhang J. EIF3i regulation of protein synthesis, cell proliferation, cell cycle progression, and tumorigenesis. Cancer Lett 2021; 500: 11-20.
[18] Blad CC, Ahmed K, Ijzerman AP and Offermanns S. Biological and pharmacological roles of HCA receptors. Adv Pharmacol 2011; 62: 219-250.
[19] Simonetti A, Brito Querido J, Myasnikov AG, Mancera-Martinez E, Renaud A, Kuhn L and Hashem Y. EIF3 peripheral subunits rearrangement after mRNA binding and start-codon recognition. Mol Cell 2016; 63: 206-217.
[20] Yuan Y, Zhang Y, Yao S, Shi H, Huang X, Li Y, Wei Y and Lin S. The translation initiation factor eIF3i up-regulates vascular endothelial growth factor a, accelerates cell proliferation, and promotes angiogenesis in embryonic development and tumorigenesis. J Biol Chem 2014; 289: 28310-28323.